

Supporting Information

Induction of mTOR-dependent Autophagy by WS₂ Nanosheets from both Inside and Outside of Human Cells

Xiaofei Zhou^{a,b}, Bing Yan^{a,c,*}

^a Institute of Environmental Research at Greater Bay, Key Laboratory for Water Quality and Conservation of the Pearl River Delta, Ministry of Education, Guangzhou University, Guangzhou 510006, China

^b School of Chemistry and Chemical Engineering, Shandong University, Jinan, 250100, China

^c School of Environmental Science and Engineering, Shandong University, Jinan 250100, China

* To whom correspondence should be addressed.

E-mail: drbingyan@yahoo.com

Contents

1. Figure S1. Photos of WS₂-4 and WS₂-30 in water and cell culture medium after staying for three days.
2. Figure S2. No obvious cell damage induction by WS₂-4 or WS₂-30 below 4 cm²/mL in 16HBE cells.
3. Figure S3. No obvious cellular oxidative stress induction by WS₂-4 or WS₂-30 in 16HBE cells.
4. Figure S4. Time-dependent LC3-II formation induced by WS₂-4 in 16HBE cells.
5. Figure S5. Supernatant of WS₂-4 or WS₂-30 had no relation to cell autophagy induction.
6. Table S1. Fold up- or down-regulation of 84 autophagic genes by super array.

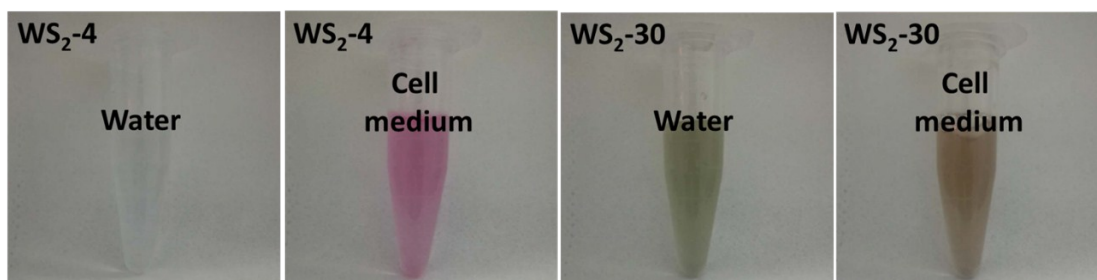


Figure S1. Photos of WS₂-4 and WS₂-30 in water and cell culture medium after staying for three days.

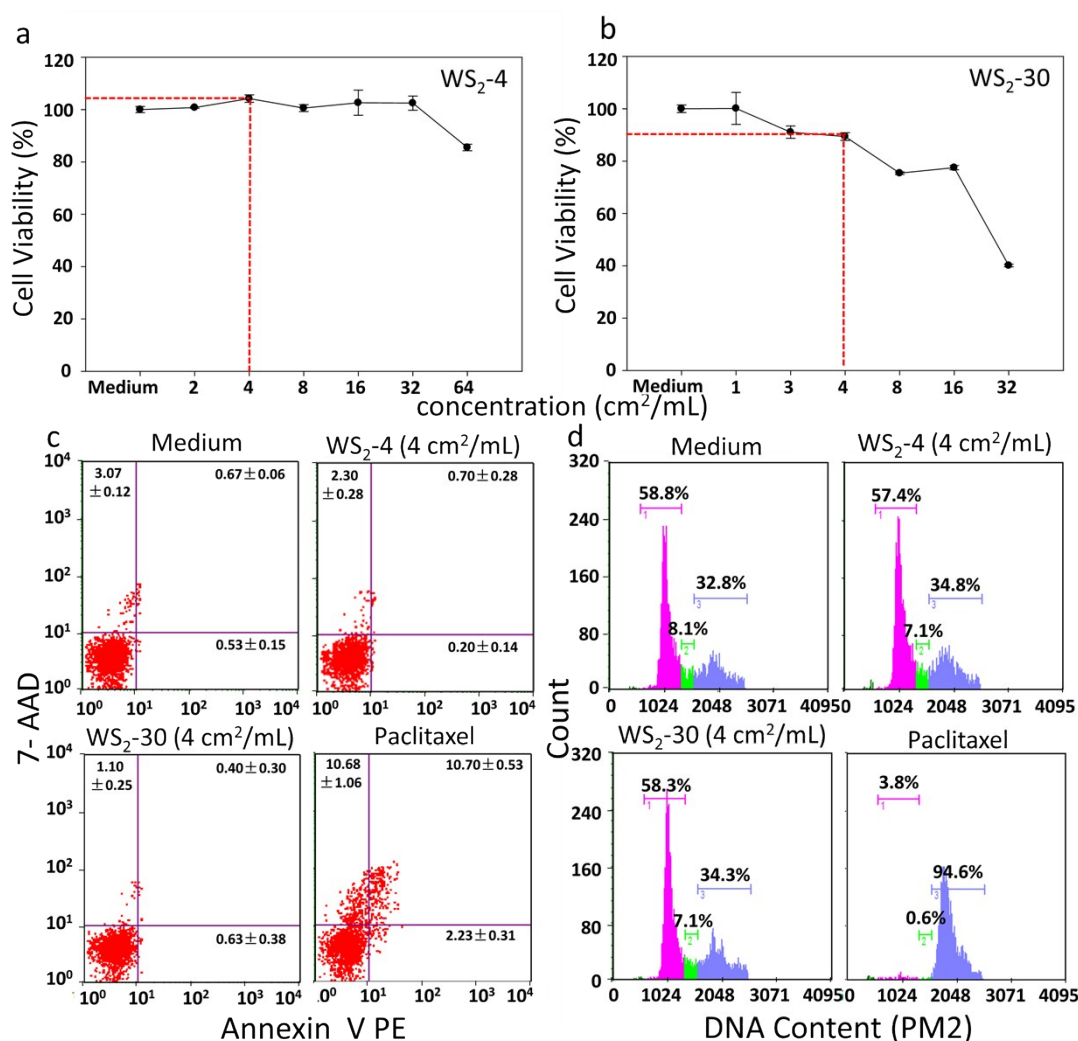


Figure S2. No obvious cell damage induction by WS₂-4 or WS₂-30 below 4 cm²/mL in 16HBE cells. (a, b) Dose-dependent cytotoxicity of WS₂-4 (a) or WS₂-30 (b) in 16HBE cells. (c) Apoptosis induced by WS₂-4 or WS₂-30 in 16HBE cells. Cells treated with cell culture medium or paclitaxel 100 nM for 12 h were used as negative or positive control. (d) Cell cycle arrest induced by WS₂-4 or WS₂-30 in 16HBE cells. 16HBE cells treated with cell culture medium or paclitaxel 1 μM for 12 h were used as negative or positive control.

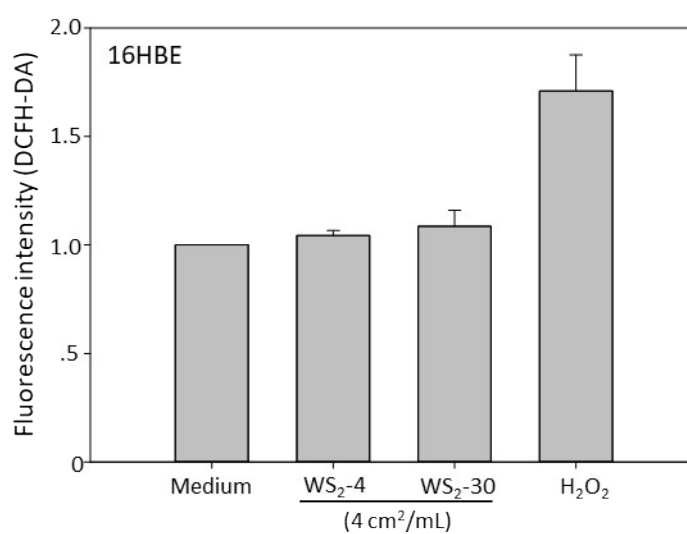


Figure S3. No obvious cellular oxidative stress induction by WS₂-4 or WS₂-30 in 16HBE cells. Cellular oxidative stress was measured after 16HBE cells were incubated with WS₂-4 or WS₂-30 at 4 cm²/mL for 12 h by DCFH-DA assay. H₂O₂ (500 μ M) or cell culture medium was respectively used as positive or negative control. Data were shown as mean \pm s.d. (n = 3).

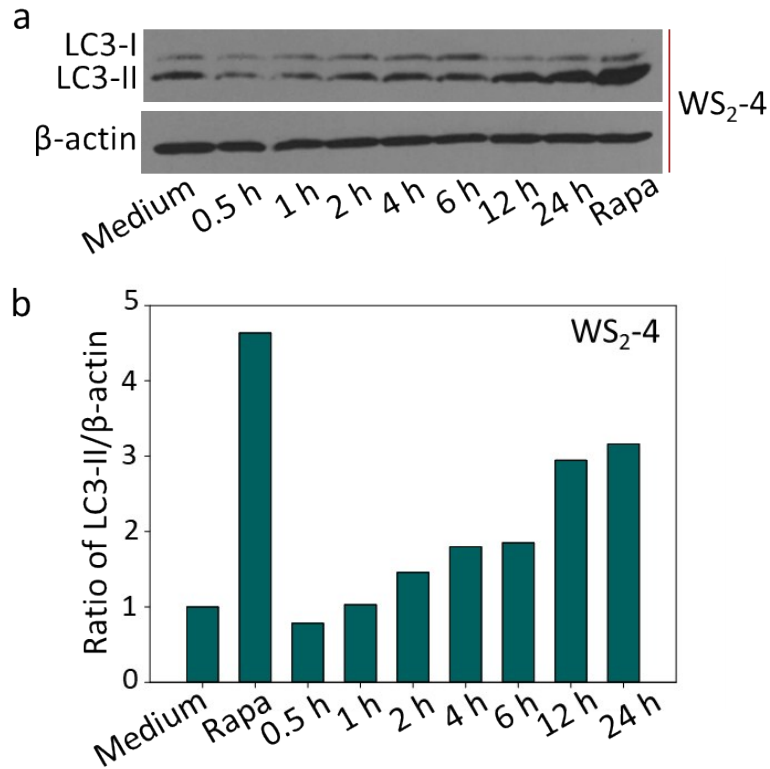


Figure S4. Time-dependent LC3-II formation induced by WS₂-4 in 16HBE cells. (a) Time-dependent LC3-II formation after treatment with WS₂-4 at a concentration of 4 μ M as determined by Western blotting against LC3B antibody in 16HBE cells. Rapamycin (10 μ M) or cell culture medium were used as positive or negative controls. (b) WS₂-4 induced time-dependent LC3-II formation in 16HBE cells was quantified by the intensity ratio of LC3-II over β -actin bands using ImageJ.

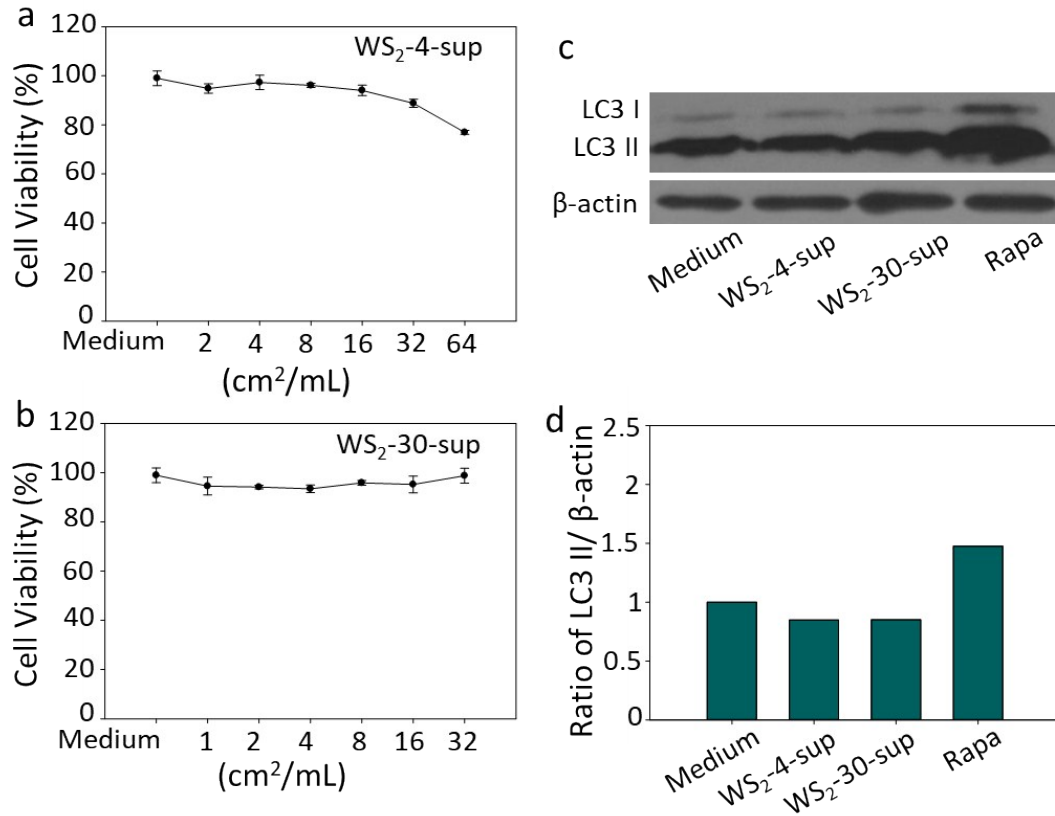


Figure S5. Supernatant of WS₂-4 or WS₂-30 had no relation to cell autophagy induction. (a, b) Dose-dependent cytotoxicity of supernatant of WS₂-4 (a) or WS₂-30 (b) in 16HBE cells. (c) LC3-II formation after treatment with the supernatant of WS₂-4 or WS₂-30 in 16HBE cells as determined by Western blotting against LC3B antibody. Cells treated with rapamycin (10 μ M) or cell culture medium for 12 h was used as the positive or negative control. (d) LC3-II formation induced by the supernatant of WS₂-4 or WS₂-30 was quantified by the ration of band intensity of LC3-II to β -actin through ImageJ.

Table S1. Fold up- or down-regulation of 84 autophagic genes by super array.

Genes	WS ₂ -4/Control	WS ₂ -30/Control
AKT1	-1.32	-1.32
AMBRA1	-1.16	-1.45
APP	-1.83	-2.16
ATG10	-1.25	-1.21
ATG12	-1.11	-1.36
ATG16L1	-1.22	-1.31
ATG16L2	1.57	-1.21
ATG3	1.07	-1.35
ATG4A	-1.04	-2.41
ATG4B	1.29	-1.10
ATG4C	-1.81	-1.41
ATG4D	1.30	-1.71
ATG5	-1.61	-1.49
ATG7	-1.17	-1.28
ATG9A	-1.41	-1.68
ATG9B	-1.72	3.47
BAD	1.20	-1.95
BAK1	-1.01	-1.82
BAX	-1.13	-1.31
BCL2	-2.08	-3.71
BCL2L1	-1.46	-1.44
BECN1	1.19	-1.27
BID	-1.77	-1.74
BNIP3	1.24	-1.61
CASP3	-2.04	-1.72
CASP8	-1.26	-1.51
CDKN1B	-1.15	-2.12
CDKN2A	1.42	-1.35
CLN3	-1.48	-2.03
CTSB	1.07	-1.43
CTSD	-1.04	-1.42
CTSS	1.88	-1.02
CXCR4	-2.11	-1.35
DAPK1	-1.13	-2.01
DRAM1	-1.94	-1.64
DRAM2	-1.46	-2.27
EIF2AK3	-2.01	-1.51

EIF4G1	-1.44	-1.25
ESR1	-4.17	-1.20
FADD	-1.21	-1.64
FAS	-1.83	-1.55
GAA	1.16	-1.84
GABARAP	1.04	-1.40
GABARAPL1	-1.25	-1.00
GABARAPL2	-1.49	-1.66
HDAC1	1.45	-1.47
HDAC6	1.24	1.23
HGS	-1.15	-1.20
HSP90AA1	-2.33	-2.58
HSPA8	-1.77	-2.17
HTT	1.07	-1.10
IFNG	1.42	-1.35
IGF1	-4.45	-1.35
INS	1.15	-1.35
IRGM	1.42	-1.35
LAMP1	-1.11	-1.24
MAP1LC3A	-2.92	-1.39
MAP1LC3B	-1.72	-1.10
MAPK14	-2.74	-1.63
MAPK8	-2.55	-1.77
MTOR	-1.12	-1.02
NFKB1	-1.46	-1.19
NPC1	-4.01	1.10
PIK3C3	-1.56	-2.27
PIK3CG	2.19	-1.35
PIK3R4	-2.34	-1.50
PRKAA1	-2.21	-1.77
PTEN	-1.10	-2.38
RAB24	-1.31	-2.08
RB1	-2.03	-3.11
RGS19	-1.43	-1.86
RPS6KB1	-2.01	-1.78
SNCA	-1.05	-2.49
SQSTM1	1.12	1.09
TGFB1	-1.64	-1.78
TGM2	-1.13	1.06
TMEM74	-1.45	-2.77
TNF	2.91	1.30
TNFSF10	-1.13	-3.35
TP53	1.12	1.10

ULK1	1.69	1.26
ULK2	-1.63	-1.37
UVRAG	-2.25	-1.60
WIPI1	-1.06	-1.10
ACTB	1.05	1.25
B2M	-1.29	-1.72
GAPDH	1.35	-1.05
HPRT1	-1.22	-1.41